SAE TECHNICAL PAPER SERIES

2002-01-0540

Low Speed Collinear Impact Severity: A Comparison between Full Scale Testing and Analytical Prediction Tools with Restitution Analysis

A. L. Cipriani, F. P. Bayan, M. L. Woodhouse, A. D. Cornetto, A. P. Dalton, C. B. Tanner and T. A. Timbario
FTI/SEA Consulting

E. S. Deyerl
Quan, Smith & Associates

Reprinted From: Accident Reconstruction 2002 (SP–1666)

The Engineering Society For Advancing Mobility Land Sea Air and Space®
INTERNATIONAL

SAE 2002 World Congress
Detroit, Michigan
March 4-7, 2002

400 Commonwealth Drive, Warrendale, PA 15096-0001 U.S.A. Tel: (724) 776-4841 Fax: (724) 776-5760

ISSN 0148-7191

Printed in USA

2002-01-0540

Low Speed Collinear Impact Severity: A Comparison Between Full Scale Testing and Analytical Prediction Tools with Restitution Analysis

A. L. Cipriani, F. P. Bayan, M. L. Woodhouse, A. D. Cornetto, A. P. Dalton, C. B. Tanner and T. A. Timbario
FTI/SEA Consulting

E. S. Deyerl
Quan, Smith & Associates

ABSTRACT

Low speed collinear collisions have received some attention in the past in published technical literature. Underrepresented are full-scale instrumented tests utilizing vehicles equipped with foam core bumpers and closing speeds greater than 2.2 meters per second (m/s). Systematic testing was designed to obtain data in collisions between vehicles with similar and mixed bumper structures. Testing was performed at closing speeds ranging from 0.8 to 5.4 m/s. Following each test, vehicle bumper and other damage was documented. Data from the 30 tests for each category of bumper and mixed categories were analyzed to identify the test speed, load magnitude, velocity change, duration of impact and coefficient of restitution. In addition, the energy absorption characteristics and damage thresholds of the various types of bumper systems were obtained. The coefficient of restitution was analyzed as a function of closing speed, velocity change, impact duration, bumper type, and other parameters and compared to previously published data and equations. A modified momentum-energy-restitution (MER) method was also used to calculate predicted vehicle response for each test and compare it to the actual test results.

INTRODUCTION

Much has been published and conjectured about the difference in behavior of foam core and piston absorber bumper systems, but there is relatively little full scale, low-speed testing data available for vehicles equipped with foam core bumpers. One of the goals of this series of tests was to document the low-speed impact behavior of foam core bumper systems and their interaction with other foam core and piston absorber systems. These results can then be correlated with previously published tests and analysis.

One difference in analyzing low-speed collisions versus high-speed impacts is the inclusion of the effects of restitution. The coefficient of restitution is a measure of the rebound that occurs when a vehicle strikes another object. Mathematically, it is the ratio of separation velocity and closing velocity. A restitution value of one reflects a purely elastic impact, which cannot occur in real world vehicle-to-vehicle collisions. Zero restitution indicates a purely plastic impact. A small or zero restitution typically occurs at higher speeds or when the vehicles remain interlocked post-impact as in some under-ride type collisions. Several existing publications provided restitution values for various vehicle-to-vehicle and vehicle-to-barrier impacts, primarily with piston absorber bumper systems. The goals of this paper are to expand the restitution data for vehicle-to-vehicle impacts, to compare these data to the correlation presented by Antonetti [1], and to incorporate and analyze data from various tests as documented in various references [2-6]. A new correlation was developed using the data from the testing performed by the authors combined with data previously presented by Antonetti [1] and others [2-6]. In addition, correlations are presented for piston absorber to piston absorber impacts and foam core to foam core impacts separately.

One way to predict a vehicle's response to a low-speed collision is by way of the MER method. This method uses restitution data and energy from barrier data to determine velocity change. Bailey, et al's [7] previous work compared velocity change calculated by the MER method to velocity change from staged low-speed impacts. Bailey, et al also measured average isolator compression in specific vehicle-to-vehicle impacts. In Bailey, et al's [7] paper, the average isolator compression was compared to actual vehicle-to-barrier impacts to determine energy and restitution.

In accident reconstruction, the question often posed is whether collision severity is sufficient to cause certain injuries to the occupants of the vehicles. The first step in such an analysis is to determine the severity of the impact in terms of velocity change, average acceleration, and peak acceleration. The ultimate question about injuries is the domain of the biomechanical engineer and will not be addressed in this paper. In many low-speed collisions a specific level of severity cannot be precisely determined. This is particularly true when no permanent crush can be identified or when only photographs and repair estimates are available. However, an upper limit modified MER analysis can be undertaken. In such an analysis, a maximum velocity change is calculated by using conservative estimates of all parameters lacking precise values. One method of performing such an analysis is detailed in the following steps:

- Determine the appropriate vehicle weights including occupants and loads. A conservative approach to incomplete weight data will minimize the weight of the vehicle of interest and maximize the other.

- Calculate vehicle stiffness coefficients, "A" and "B", for the year, make, and model group of vehicles to determine the crush energy involved. Assume an extent of crush that is conservative, and include some minimal amount of permanent crush in cases where none appears in photographs or repair estimates. In addition, using the maximum possible width for the contact area will also maximize velocity change.

- Compare the force of impact computed for each vehicle. The force at impact must be equal for each vehicle, but cannot exceed the smaller of the two.

- Use the appropriate restitution for the relative approach or closing speed at impact. This is an iterative process, which will converge on the calculated upper limit for velocity change.

- The average acceleration can then be obtained by dividing the velocity change by a minimum impact duration of 100 milliseconds (msec). Assuming a half triangle wave, the peak acceleration is simply 2 times the average acceleration.

The presented method varies from Bailey; et al in that energy is calculated by way of bumper stiffness' ("A" and "B" coefficients) from crash tests performed by the Department of Transportation (DOT) and other published sources. Data sources such as Neptune's compilation [8] and crash plots using the Campbell [9] or Prasad [10] methods may also be used. The presented method offers an upper limit to velocity change, average acceleration, and peak acceleration. This paper also compares calculated values using the above method with the actual test values of velocity change, average acceleration, and peak acceleration. Correlation between the results will validate the use of this modified MER method as a means to determine an upper limit vehicle response in low-speed collisions.

FULL SCALE TESTING

TEST PROCEDURE

A matrix of 30 low-speed collinear collisions were staged using 4 different test vehicles: 2 with foam core bumper systems and 2 with piston absorber systems. Tests were conducted with the front of the bullet vehicle impacting the rear of the target vehicle. The matrix was assembled as follows: piston absorber into piston absorber, foam core into foam core, piston absorber into foam core, and foam core into piston absorber. The vehicles consisted of a 1986 Honda Accord, a 1988 Mazda 929, a 1989 Chevrolet Cavalier, and a 1985 Chevrolet Celebrity. The bullet and target vehicles were interchanged so that each vehicle's front and rear bumpers were tested up to the 5.4 m/s closing speed. The bullet vehicle speed was increased by propelling it to the desired speed measured via radar gun and 5th wheel until impact with the target. The target vehicle brakes were released and this vehicle was allowed to roll freely. In some of the higher speed tests, the vehicle was brought to a controlled rest. The bullet vehicle was released just prior to impact. The test matrix was designed to test vehicles at speed increments of 0.8 m/s to approximately 5.4 m/s. Table 1 presents the actual tested speeds.

Table 1. Testing Matrix.

Test #	Bullet	Target	Actual Speed (m/s)
1-7	Honda	Mazda	0.9, 0.8, 1.6, 2.9, 4.1, 4.6, 5.0
8-10	Mazda	Honda	0.9, 2.1, 2.5
11-15	Mazda	Cavalier	1.1, 1.7, 3.1, 4.0, 4.9
16-21	Cavalier	Celebrity	0.8, 1.7, 2.9, 3.8, 4.2, 5.8
22-24	Celebrity	Cavalier	0.8, 1.7, 2.7
25-27	Mazda	Honda	3.7, 4.6, 5.2
28-30	Celebrity	Cavalier	3.7, 4.6, 5.8

TEST VEHICLES

The 4 test vehicles were inspected, weighed, and documented photographically and geometrically prior to testing. The requirements for selecting the vehicles were that they be fairly common and generally representative of the average passenger car, be capable of rolling freely, have all major components such as engines, interiors, and transmissions in place, and that they have undamaged front and rear bumper structures. The vehicles were unaltered prior to testing and all fluids were drained. Table 2 shows each vehicle's specifications. Appendix A provides a more complete listing of test vehicle data including an illustrated parts diagram of each bumper system. The "A" and "B" values presented in Table 2 were calculated using the Campbell [9] and Prasad [10] methods. The method that produced the best correlation result was used.

Table 2. Vehicle Specifications.

	Honda	**Mazda**	**Cavalier**	**Celebrity**
Type	Sedan	Sedan	Coupe	Sedan
Bumper	Foam	Foam	Piston	Piston
OAL (m)	4.57	4.90	4.55	4.78
OAW (m)	1.70	1.70	1.68	1.75
Weight (kg)	1146	1495	1052	1249
Front "A" (lb/in)	232.1	278.1	213.8	203.0
Front "B" (lb/in^2)	75.6	79.1	58.0	52.9
Rear "A" (lb/in)	156.2	352.7	227.3	197.4
Rear "B" (lb/in^2)	32.1	133.5	65.5	60.2

INSTRUMENTATION

Tri-Axial Accelerometer

The primary means of data collection for the tests was two IST EDR-3 tri-axial accelerometers. These units are self-contained "black boxes" which require no external connections during the testing sequences. One EDR-3 was mounted in each vehicle during testing. They were rigidly mounted to the transmission tunnel along the centerline, near the center of gravity of each vehicle. Each was mounted horizontally and as close to level as possible. A sampling frequency of 3.2 kHz was set for each channel. Acceleration data in the X, Y, and Z directions were recorded for analysis. A full series of tests was run with a vehicle acting as a bullet and another as the target before the data was downloaded from the EDR's to a laptop computer. The units were then moved to new vehicles for the next series of tests. This data storage capability greatly simplified and expedited the testing process. Each EDR was calibrated prior to crash testing.

The EDR units were triggered to record 500 msec of data before and after detecting a peak acceleration of 0.5 g's in any of the three axes. The units recorded a total of 1 second of data for each test collision.

Figure 1 shows overlaid sample data from the two EDR's from the full scale testing. The figure shows data from only the X direction and indicates that one vehicle had a positive acceleration (the target) while the other vehicle had a negative acceleration (the bullet).

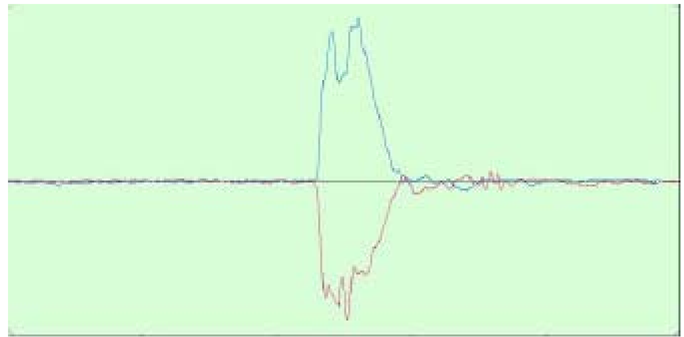

Figure 1. Sample IST Accelerometer Data.

5th Wheel

A 5th wheel was constructed using the frame and tire from a 0.50 meter unicycle with the pedals and seat removed. The shaft of the unicycle wheel was coupled to the input shaft of a 60 pulse per revolution optical encoder that served as the input to a Shimpo model DT-5TG digital tachometer. In addition to providing a digital readout, this tachometer has the ability to generate a rapidly updated analog signal proportional to its input. In addition, the unit is programmable to allow scale factors to be input for both the digital readout and the analogue output.

The 5th wheel was calibrated by measuring the distance traveled by the tire when it was rolled through a single revolution. This distance represented the travel distance of the 5th wheel for one revolution, or 60 pulses, of the optical encoder.

The unicycle frame was attached by lightweight tubing to a separate frame that mounted to the passenger's side door of each bullet vehicle through suction cups. The frames were adjustable so that the axis of the unicycle wheel could be kept parallel to the plane of the ground for all of the vehicles. In addition, there were joints in the frame that allowed the unicycle frame to rotate about pitch and yaw axes so that good wheel contact could be maintained during vehicle maneuvering.

The 5th wheel directly measured the instantaneous velocity of the bullet vehicle as it was being pushed up to impact speed, and displayed the speed to the nearest tenth of a mile per hour. This allowed the impact speed to be generally controlled in each of the tests. In addition the analog output of the device gave a record of the bullet vehicle speed going into and coming out of the impact. Data were collected by way of LabTech Notebook data acquisition software. Figure 2 is an example of 5th wheel data acquired during testing.

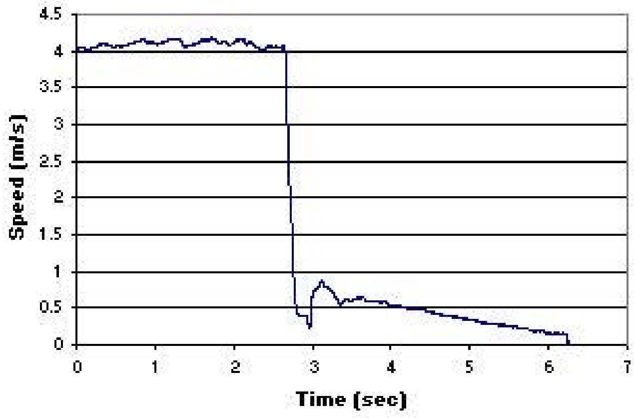

Figure 2. Sample 5^{th} Wheel Data.

Radar Gun

A Stalker ATS Profession Sports Radar gun was used to also track the closing speed of the bullet. The Radar gun was calibrated prior to crash testing using the manufacturers recommended procedures.

Photographs and Measurements

After each test the front of the bullet vehicle and the rear of the target vehicle were photographically documented. Appendix B provides a set of representative photographs from these tests. In addition, the vehicle's overall length was measured after each test to determine if any permanent crush resulted from testing. No repairs were made to the vehicles between tests.

DATA REDUCTION

Two different methods were used to reduce the data recorded by the IST accelerometers. The first method utilized the DynaMax software that accompanied the accelerometers. A 4^{th} order phaseless Butterworth filter was applied to the raw data in the direction of travel to remove noise and vibration.

The second method used DADiSP 4.0 numerical method software to integrate the acceleration data. The raw data were filtered by way of a moving average to remove noise and vibration. Acceleration data were also offset to remove any error from non-level mounting of the accelerometers. Impact duration and velocity change were determined for each test and compiled. Figure 3 shows an example of the DADiSP 4.0 output.

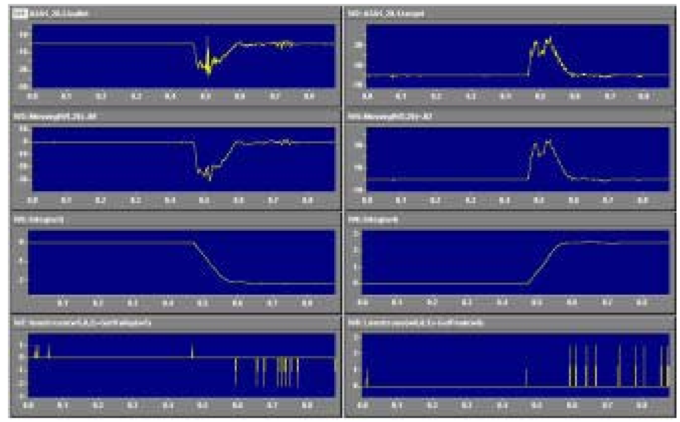

Figure 3. Sample DADiSP 4.0 Graphs.

The various recording devices provided a clear indication of the initial impact time reference. The separation time of the vehicles was distinguished using filtering or averaging of the data. The test data were viewed in the unfiltered or un-averaged format and the target and bullet vehicle data were compared to obtain the separation time. Determination of Impact duration and velocity change for each collision were then compiled and are shown in Appendix C.

Test 1 was not used for restitution or MER analysis as the target vehicle's brakes were inadvertently engaged, thus affecting the results.

ANALYSIS

RESTITUTION ANALYSIS

In reviewing Antonetti's paper, a marginally better fit to the data was discovered by using a 3^{rd} order logarithmic fit. This fit provided a better match to the data at low approach speeds above 0.25 m/s. Below 0.25 m/s, the logarithmic fit goes to infinity. A comparison of these fits is shown in Figure 4 of Appendix D. The correlation coefficient for the logarithmic fit is 0.906 whereas the exponential fit coefficient is 0.904. The equation for Antonetti's original fit and the new logarithmic fit are as follows:

$$e = 0.5992\ \exp^{-0.2508v + 0.01934v^2 - 0.001279v^3}$$

$$e = 0.47949 - 0.274781\ \log(v) - 0.07673\ \log(v)^2 - 0.01895\ \log(v)^3$$

Each of the 30 collisions provided additional data that were added to the data presented by Antonetti [1]. Third order exponential and logarithmic fits were explored. A graph of the comparison between the 3^{rd} order exponential and logarithmic best-fit curves can be seen in Figure 5. The data were also examined individually for each bumper system. Figure 6 shows 3^{rd} order logarithmic curve fits for foam core bumper systems, piston absorber bumper system, and all data. The piston type absorber data was over-represented and tends to pull the all data curve close to the piston type absorber curve. As expected, the trend illustrates restitution increases as closing speed decreases. The foam core type bumper systems tend to produce a higher restitution than the piston type absorbers. The correlation coefficient, r, for the all data curve fit is 0.806, for the form core data is 0.911, and for the piston type absorber is 0.866.

In general, the data confirmed the overall curve fit, whether in exponential or logarithmic form, produced by Antonetti [1]. Additionally, the logarithmic fit for the foam core data produces a good correlation to the available data. The following three equations were obtained from the best-fit curves:

Piston Composite (Piston to Piston)

$$e = 0.44871 - 0.24963\ \log(v) + 0.04988\ \log(v)^2 - 0.12660\ \log(v)^3$$

Foam Core Composite (Foam Core to Foam Core)

$$e = 0.53391 - 0.31054\ \log(v) + 0.22723\ \log(v)^2 - 0.28015\ \log(v)^3$$

All Data Composite

$$e = 0.47477 - 0.26139\ \log(v) + 0.03382\ \log(v)^2 - 0.11639\ \log(v)^3$$

MER METHOD COMPARISON

The MER method is a method used in reconstructing low-speed collinear collisions. The data from the 30 staged tests were compared to an analysis of each of these collisions using photographically estimated vehicle damage and the MER equations shown below:

Conservation of Momentum

$$m_T v_T + m_B v_B = m_T v_T' + m_B v_B'$$

Conservation of Energy

$$\frac{1}{2} m_T v_T^2 + \frac{1}{2} m_B v_B^2 = \frac{1}{2} m_T v_T'^2 + \frac{1}{2} m_B v_B'^2 + E_T + E_B$$

Coefficient of Restitution

$$v_T' - v_B' = e(v_B - v_T)$$

Crush Energy

$$E = L(AC + \frac{BC^2}{2} + \frac{A^2}{2B})$$

Target Vehicle Delta-V

$$\Delta v_T = \frac{(1+e)}{1 + \frac{m_T}{m_B}} \sqrt{\frac{2(E_T + E_B)(m_T + m_B)}{(1-e^2) m_T m_B}}$$

Crush Force

$$F = AL + BLC$$

Relative Approach Velocity

$$v_{RA} = \frac{1 + \frac{m_T}{m_B}}{(1+e)} \Delta v_T$$

This modified MER procedure was used for each crash test and compared to the data collected during the staged collisions. The 30 staged crash tests showed an impact duration, delta-t, of 0.098 to 0.215 seconds. No correlation was found between approach speed, velocity change, or damage and Impact duration.

Several methods can be used to calculate the peak acceleration experienced by the vehicles in a low-speed collision. The first method simply utilizes the peak force and divides by the weight of the vehicle in question, in accordance with Newton's Second Law. The second and third methods assume the shape of the impact pulse as either a half sine wave or half triangle wave. The average of both waves are 0.636 and 0.50, respectively. The peak acceleration is then calculated by dividing the average acceleration by either value. The authors determined that the only method that consistently over-predicts the peak acceleration relative to the tests was to assume a half triangle wave. The peak acceleration is twice the average acceleration.

The results of the comparison between actual crash data and the predicted modified MER values indicate an over-prediction in velocity change, average acceleration, and peak acceleration by the modified MER method as can be seen in Appendix C. Accordingly, this data verifies that the modified MER method can be used as a tool in determining the upper limit of velocity change, average acceleration, and peak acceleration in low-speed collisions under these conditions.

Predicting the precise velocity change, average acceleration, and peak acceleration in low-speed collisions with accuracy is typically difficult, if not impossible, given the limitations of data available from the real world crash. Even in an ideal case, a staged crash test with identical vehicles may not yield identical results to those of an actual collision. According, the modified MER method described herein provides an effective technique to analyze low-speed collisions. The results of such an analysis provide an upper limit value for velocity change or acceleration.

CONCLUSION

Low speed crash testing was performed to evaluate restitution of different bumper constructions, especially foam core type bumpers. The overall correlation of restitution to closing speed put forward by Antonetti [1] is considered valid with minor modifications. A 3rd order logarithmic fit appears to provide a minor improvement in correlation overall, and appears to fit much better at closing speeds of 0.25 to 1.25 m/sec. In addition, this paper provides a separate 3rd order logarithmic curve for the foam core to foam core bumper collision. The correlation of this curve to the data is considered to be good and usable for future analysis needs. More test data would further refine these correlations.

A modified MER method of analysis is presented. This method allows the analyst to determine an upper limit value for velocity change, average acceleration, and peak acceleration. When compared to the 30 crash tests performed during this study, the modified MER method always over-predicted these parameters. This method accordingly provides an effective technique to analyze low-speed collisions.

ACKNOWLEDGMENTS

The authors would like to thank Vincent Antonetti for all his help and providing data and software for data analysis and Gregory Hoshal at IST.

REFERENCES

1. Antonetti, V.W., “Estimating the Coefficient of Restitution of Vehicle-to-Vehicle Bumper Impacts”, SAE 980552.
2. Howard, R.P., Bomar, J., and Bare, C., “Vehicle Restitution Response in Low Velocity Collision”, SAE 931842.
3. Malmsbury, R.N. and Eubanks, J.J., “Damage and/or Impact Absorber (Isolator) Movements Observed in Low Speed Crash Test Involving Ford Escorts”, SAE 940912.
4. Siegmund, G.P., King, D.P., and Montgomery, D.T., “Using Barrier Impact Data to Determine Speed Change in Aligned, Low Speed Vehicle-to-Vehicle Collisions”, SAE 960887.
5. Siegmund, G.P., Bailey, M.N., and King, D.J., “Characteristics of Specific Automobile Bumpers in Low-Velocity Impacts”, SAE 940916.
6. Szabo, T.J. and Welcher, J., “Dynamics of Low Speed Crash tests with Energy Absorbing Bumpers”, SAE 921573.
7. Siegmund, G.P., Bailey, M.N., and King, D.J., “Automobile Bumper Behavior in Low-Speed Impacts”, SAE 930211.
8. http://www.neptuneeng.com
9. Campbell, K.L., “Energy Basis for Collision Severity”, SAE 740565.
10. Prasad, A.K., “Energy Dissipated in Vehicle Crush-A Study Using the Repeated Test Technique”, SAE 900412.

CONTACT

Alfred L. Cipriani, P.E. or Fawzi P. Bayan, P.E.
Principal Mechanical Engineer
Vehicle Accident Reconstructionist
FTI/SEA Consulting
1110 Benfield Boulevard
Millersville, MD 21108
(800) 635-9507

SYMBOLS

“T” and “B” subscripts denote target and bullet vehicles respectively.

m mass of vehicle

v pre-impact velocity of vehicle

v' post-impact velocity of vehicle

e intervehicular restitution

E energy

A crush coefficient

B crush coefficient

C depth of crush

L length of crush

Δv change in velocity of vehicle

F crush impact force

Appendix A

1986 Honda Accord 4 Door Sedan
VIN: JHMBA7430GC044106

1986 Honda Accord LX Sedan

FRONT BUMPER

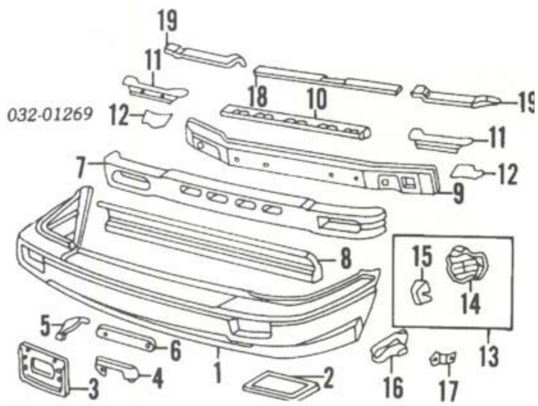

1986 Honda Accord LX Sedan

REAR BUMPER

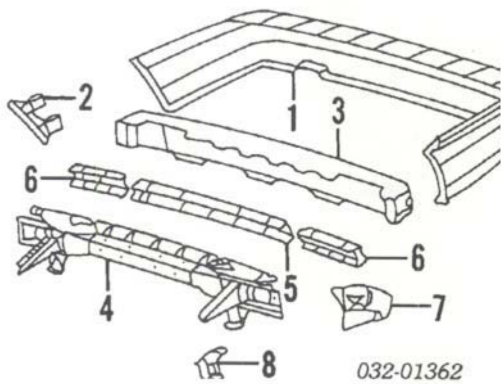

1988 Mazda 929 4 Door Sedan
VIN: JM1HC221XJ0101575

1988 Mazda 929 (none) Sedan

FRONT BUMPER

35-799

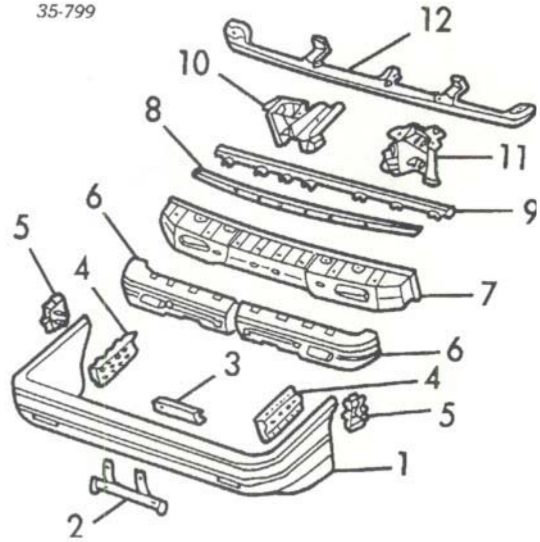

1988 Mazda 929 (none) Sedan

REAR BUMPER

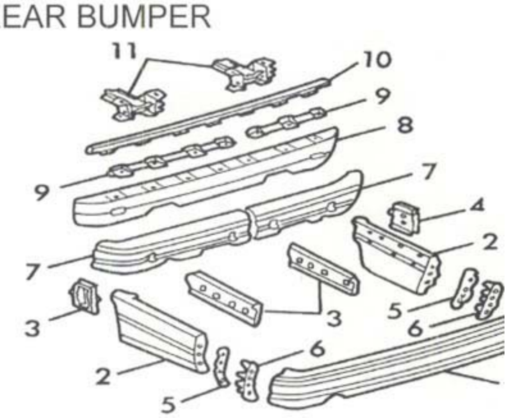

1989 Chevrolet Cavalier 2 Door Coupe
VIN: 1G1JC1114KJ299443

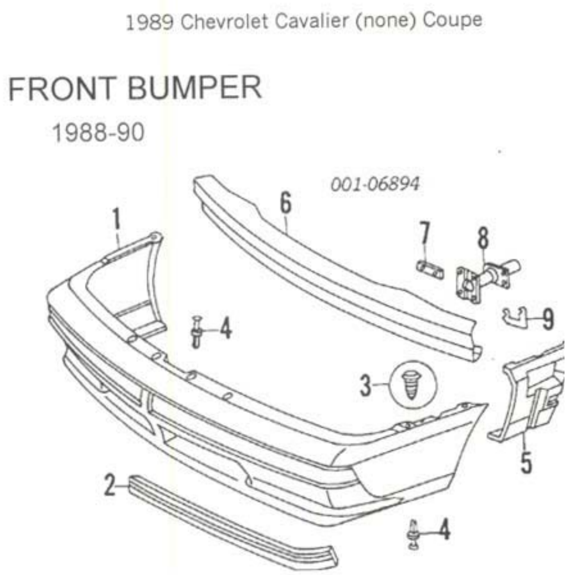

1985 Chevrolet Celebrity 4 Door Sedan
VIN: 2G1AW19R4F1209175

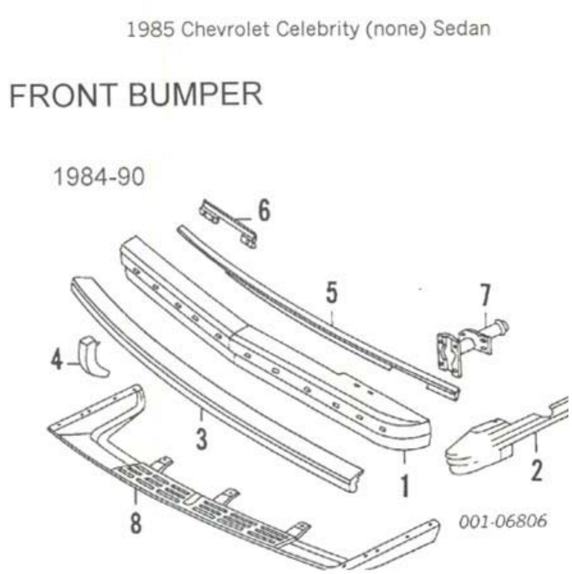

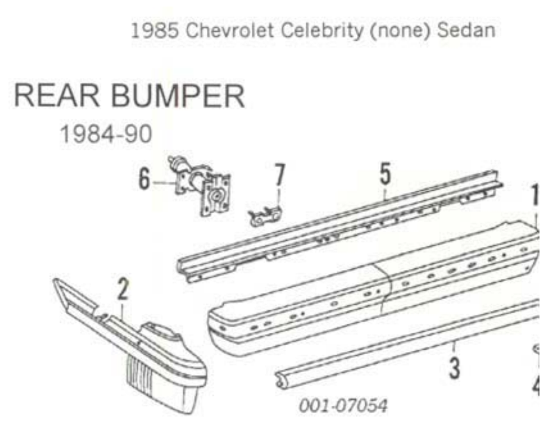

Appendix B

Photo 1. 0.8 m/s. Rear of Mazda. Minor blemishes to plastic bumper cover from Honda license plate mounting bolts. No permanent crush damage.

Photo 2. 0.8 m/s. Front of Honda. Note license plate mounting bolts. No permanent crush damage.

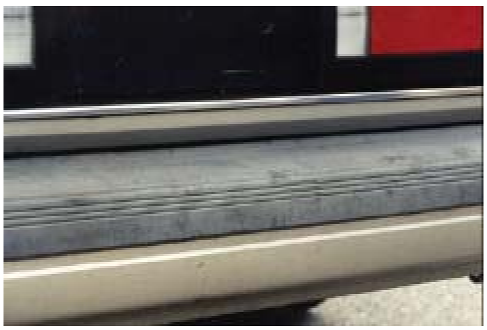

Photo 3. 1.6 m/s. Rear of Mazda. No permanent crush damage.

Photo 4. 1.6 m/s. Front of Honda. No permanent crush damage.

Photo 5. 2.9 m/s. Rear of Mazda. No permanent crush damage.

Photo 6. 2.9 m/s. Front of Honda. No permanent crush damage.

Photo 7. 4.1 m/s. Rear of Mazda. More pronounced scuffing. No permanent crush damage.

Photo 8. 4.1 m/s. Front of Honda. More pronounced scuffing. No permanent crush damage.

Photo 9. 4.6 m/s. Rear of Mazda. Bumper cover detached at right rear wheel well and bumper rotated downward slightly.

Photo 10. 4.6 m/s. Front of Honda. Permanent crush damage to left front corner of bumper.

Photo 11. 5.0 m/s. Rear of Mazda. No additional damage noted.

Photo 12. 5.0 m/s. Front of Honda. More severe damage, including buckling of engine compartment hood.

Photo 13. 0.8 m/s. Rear of Celebrity.
No permanent crush damage.

Photo 14. 0.8 m/s. Front of Cavalier.
No permanent crush damage.

Photo 15. 1.7 m/s. Rear of Celebrity.
No permanent crush damage.

Photo 16. 1.7 m/s. Front of Cavalier.
No permanent crush damage.

Photo 17. 2.9 m/s. Rear of Celebrity.
No permanent crush damage.

Photo 18. 2.9 m/s. Front of Cavalier.
No permanent crush damage.

Photo 19. 3.8 m/s. Rear of Celebrity. Right side of bumper permanently crushed inward approximately one inch.

Photo 20. 3.8 m/s. Front of Cavalier. No permanent crush damage.

Photo 21. 4.2 m/s. Rear of Celebrity. Right side of bumper permanently crushed inward approximately three inches.

Photo 22. 4.2 m/s. Front of Cavalier. Some permanent crush damage.

Photo 23. 5.8 m/s. Rear of Celebrity. Additional permanent crush damage.

Photo 24. 5.8 m/s. Front of Cavalier. Additional permanent crush damage.

Appendix C

Test #	Vehicle	V (init) (m/s)	Test DELTA Vx (m/s)	MER DELTA Vx (m/s)	Test Gx (ave) (g)	MER Gx (ave) (g)	Test Gx (peak) (g)	MER Gx (peak) (g)	Restitution	DELTA t (sec)
1	HONDA	0.9	(0.6)	N/A	(0.4)	N/A	(1.0)	N/A	0.22	0.104
1	MAZDA	0.0	0.4	N/A	0.3	N/A	0.6	N/A		0.104
2	HONDA	0.8	(0.8)	(3.4)	(0.4)	(3.4)	(1.3)	(6.8)	0.62	0.137
2	MAZDA	0.0	0.6	2.6	0.3	2.6	0.9	5.2		0.137
3	HONDA	1.6	(1.4)	(3.4)	(0.8)	(3.5)	(2.6)	(7.0)	0.54	0.124
3	MAZDA	0.0	1.0	2.6	0.6	2.7	1.8	5.4		0.124
4	HONDA	2.9	(2.2)	(3.4)	(1.5)	(3.5)	(4.5)	(7.0)	0.34	0.101
4	MAZDA	0.0	1.7	2.6	1.1	2.7	2.9	5.4		0.101
5	HONDA	4.1	(3.2)	(3.4)	(1.7)	(3.5)	(6.0)	(7.0)	0.38	0.130
5	MAZDA	0.0	2.4	2.6	1.3	2.7	4.2	5.4		0.130
6	HONDA	4.6	(3.6)	(3.6)	(2.5)	(3.6)	(7.2)	(7.3)	0.37	0.101
6	MAZDA	0.0	2.7	2.7	1.9	2.8	4.9	5.6		0.101
7	HONDA	5.0	(3.9)	(4.2)	(2.7)	(4.2)	(8.2)	(8.5)	0.35	0.098
7	MAZDA	0.0	2.9	3.2	2.0	3.3	5.4	6.5		0.098
8	MAZDA	0.9	(0.6)	(2.5)	(0.3)	(2.6)	(1.0)	(5.2)	0.50	0.119
8	HONDA	0.0	0.7	3.4	0.4	3.4	1.4	6.8		0.119
9	MAZDA	2.1	(1.4)	(2.5)	(0.8)	(2.6)	(2.5)	(5.2)	0.46	0.113
9	HONDA	0.0	1.7	3.4	1.1	3.4	3.3	6.8		0.113
10	MAZDA	2.5	(1.7)	(2.5)	(1.1)	(2.6)	(3.4)	(5.2)	0.55	0.108
10	HONDA	0.0	2.1	3.4	1.4	3.4	4.1	6.8		0.108
11	MAZDA	1.1	(0.6)	(2.4)	(0.3)	(2.5)	(0.9)	(5.0)	0.31	0.155
11	CAVALIER	0.0	0.8	3.4	0.3	3.5	1.0	7.0		0.155
12	MAZDA	1.7	(1.1)	(2.4)	(0.5)	(2.5)	(1.6)	(5.0)	0.52	0.155
12	CAVALIER	0.0	1.5	3.4	0.6	3.5	1.9	7.0		0.155
13	MAZDA	3.1	(1.8)	(2.4)	(0.8)	(2.5)	(3.1)	(5.0)	0.38	0.150
13	CAVALIER	0.0	2.5	3.4	1.2	3.5	4.0	7.0		0.150
14	MAZDA	4.0	(2.2)	(2.4)	(1.3)	(2.5)	(4.1)	(5.0)	0.34	0.119
14	CAVALIER	0.0	3.1	3.4	1.8	3.5	6.3	7.0		0.119
15	MAZDA	4.9	(2.8)	(2.9)	(1.6)	(2.9)	(5.4)	(5.8)	0.34	0.121
15	CAVALIER	0.0	3.8	4.1	2.2	4.2	6.6	8.3		0.121
16	CAVALIER	0.8	(0.8)	(3.1)	(0.3)	(3.2)	(1.0)	(6.4)	0.73	0.167
16	CELEBRITY	0.0	0.6	2.6	0.2	2.7	0.9	5.4		0.167
17	CAVALIER	1.7	(1.2)	(3.1)	(0.5)	(3.2)	(1.3)	(6.4)	0.27	0.176
17	CELEBRITY	0.0	0.9	2.6	0.4	2.7	1.3	5.4		0.176
18	CAVALIER	2.9	(1.9)	(3.1)	(0.7)	(3.2)	(2.2)	(6.4)	0.20	0.190
18	CELEBRITY	0.0	1.6	2.6	0.6	2.7	2.2	5.4		0.190
19	CAVALIER	3.8	(2.6)	(3.3)	(1.4)	(3.4)	(3.3)	(6.7)	0.25	0.128
19	CELEBRITY	0.0	2.2	2.8	1.2	2.8	3.3	5.7		0.128
20	CAVALIER	4.2	(2.9)	(3.6)	(1.7)	(3.7)	(4.2)	(7.4)	0.26	0.115
20	CELEBRITY	0.0	2.5	3.0	1.5	3.1	4.3	6.2		0.115
21	CAVALIER	5.8	(3.8)	(4.0)	(2.6)	(4.1)	(7.7)	(8.2)	0.24	0.102
21	CELEBRITY	0.0	3.3	3.4	2.3	3.5	6.9	6.9		0.102
22	CELEBRITY	0.8	(0.6)	(2.7)	(0.2)	(2.8)	(0.8)	(5.6)	0.31	0.171
22	CAVALIER	0.0	0.5	3.2	0.2	3.3	1.5	6.6		0.171
23	CELEBRITY	1.7	(1.1)	(2.7)	(0.4)	(2.8)	(1.6)	(5.6)	0.36	0.215
23	CAVALIER	0.0	1.2	3.2	0.4	3.3	1.5	6.6		0.215
24	CELEBRITY	2.7	(1.6)	(2.7)	(0.7)	(2.8)	(2.1)	(5.6)	0.26	0.166
24	CAVALIER	0.0	1.8	3.2	0.8	3.3	2.8	6.6		0.166
25	MAZDA	3.7	(2.3)	(2.8)	(1.5)	(2.9)	(4.3)	(5.7)	0.45	0.104
25	HONDA	0.0	3.1	3.7	2.0	3.7	6.7	7.5		0.104
26	MAZDA	4.6	(2.7)	(4.0)	(1.8)	(4.1)	(5.8)	(8.2)	0.40	0.107
26	HONDA	0.0	3.7	5.3	2.4	5.4	7.1	10.7		0.107
27	MAZDA	5.2	(2.9)	(4.0)	(2.0)	(4.1)	(6.4)	(8.2)	0.28	0.100
27	HONDA	0.0	3.8	5.3	2.6	5.4	8.8	10.7		0.100
28	CELEBRITY	3.7	(2.1)	(2.8)	(1.1)	(2.9)	(3.1)	(5.7)	0.26	0.128
28	CAVALIER	0.0	2.5	3.4	1.4	3.4	3.7	6.8		0.128
29	CELEBRITY	4.6	(2.8)	(3.0)	(1.2)	(3.0)	(3.7)	(6.1)	0.34	0.167
29	CAVALIER	0.0	3.4	3.5	1.4	3.6	5.2	7.2		0.167
30	CELEBRITY	5.8	(3.3)	(3.7)	(1.7)	(3.8)	(5.2)	(7.5)	0.28	0.135
30	CAVALIER	0.0	4.1	4.4	2.1	4.5	6.5	8.9		0.135

Appendix D

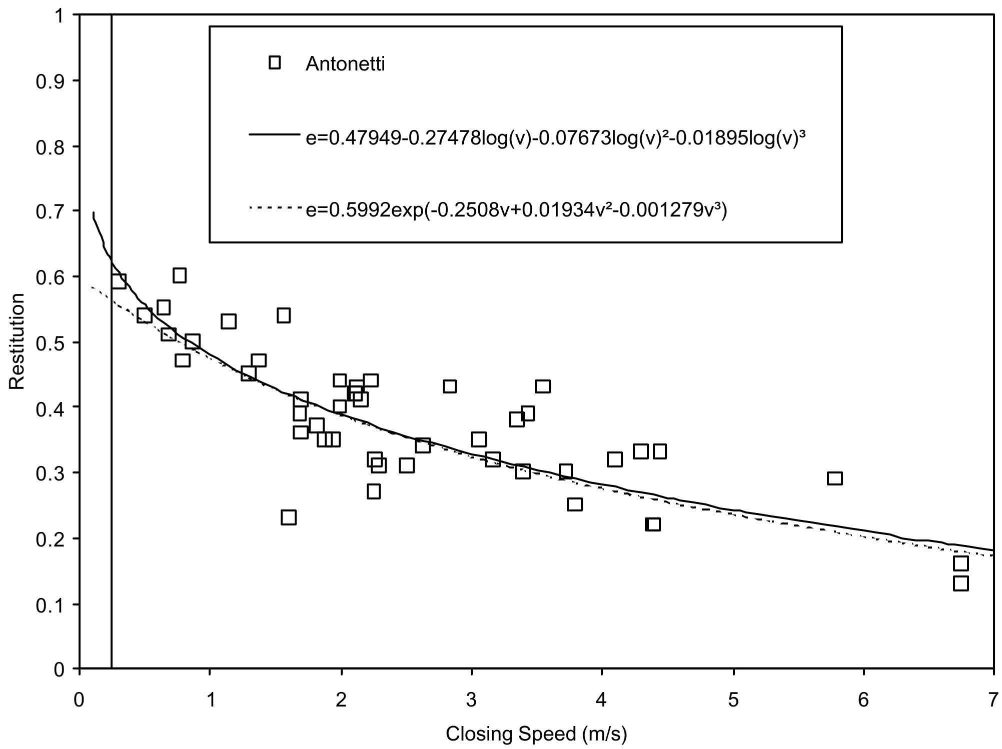

Figure 4.

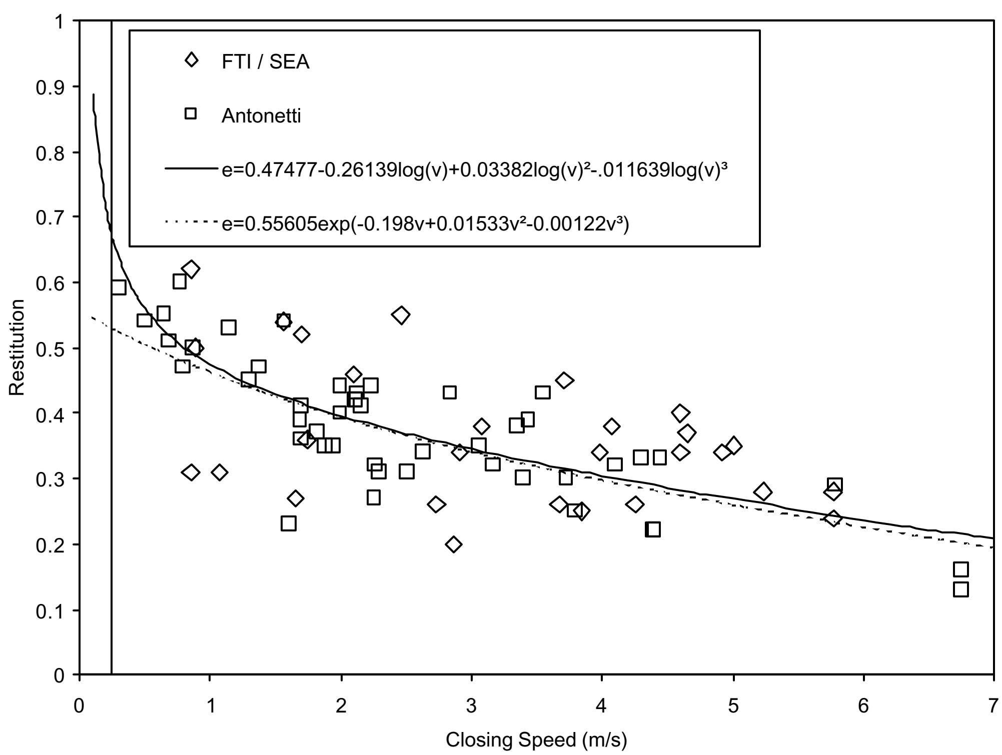

Figure 5.

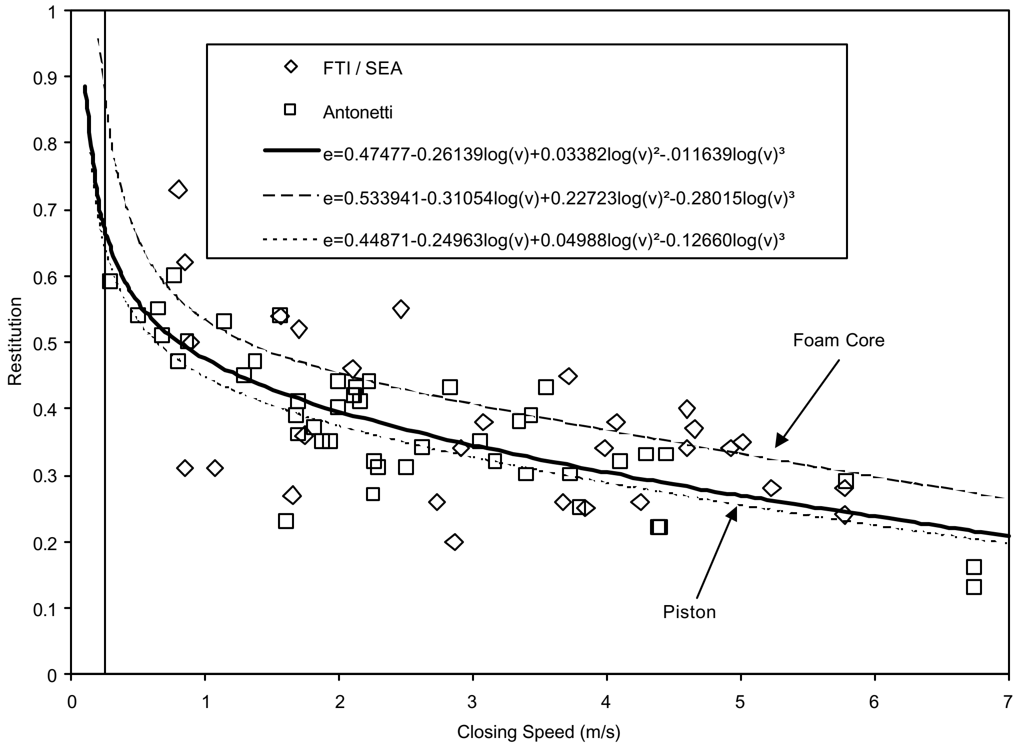
FTI / SEA
Antonetti
e=0.47477-0.26139log(v)+0.03382log(v)²-.011639log(v)³
e=0.533941-0.31054log(v)+0.22723log(v)²-0.28015log(v)³
e=0.44871-0.24963log(v)+0.04988log(v)²-0.12660log(v)³
Foam Core
Piston
Restitution
Closing Speed (m/s)
0
0.1
0.2
0.3
0.4
0.5
0.6
0.7
0.8
0.9
1
2
3
4
5
6
7

Figure 6.